Research Article

Numerical and Experimental Study on the Multiobjective Optimization of a Two-Disk Flexible Rotor System

Zheng Longxi,[1,2] Jia Shengxi,[1] and Huang Jingjing[1]

[1]*School of Power and Energy, Northwestern Polytechnical University, Xi'an 710072, China*
[2]*Collaborative Innovation Center of Advanced Aero-Engine, Beijing 100191, China*

Correspondence should be addressed to Jia Shengxi; jia_sx@163.com

With the ever-increasing requirement for the thrust to weight ratio, the rotational speed of modern aeroengine is increasingly improved; thus most of the aeroengine rotor is flexible. Some dynamic problems, such as excessive vibration, appear due to the increase of the rotation speed of the aeroengine. The aim of this study is to reduce the vibration level of the flexible rotor system through optimum design. A laboratory scale two-disk flexible rotor system representing a typical aeroengine rotor system is designed. A combinational optimization strategy coupling the rotordynamics calculation software ANSYS and the multidisciplinary optimization software ISIGHT is proposed to optimize the rotor system. The positions of the disks are selected as the design variables. Constraints are imposed on critical speeds. The disks' amplitudes and bearings' transmitted forces are chosen as the optimization objectives. Using this strategy, the optimal positions of the two disks are obtained. The numerical optimization results are verified by the experiments based on the test rig. The results show a significant vibration level reduction after optimization.

1. Introduction

In order to obtain a higher thrust to weight ratio, aeroengines are developed with higher rotation speed and lighter weight, which leads to some critical rotordynamics issues. The most important one is excessive vibration of the rotor system. The excessive vibration may result in fatigue of components and even catastrophic failure. Thus, dynamic design of the rotor system becomes increasingly onerous. Traditionally, the rotor's final structural scheme is obtained through adjusting the structural parameters manually, which is inefficient and has difficulty in achieve the best results [1]. To improve the design quality, shorten the design cycle, and meet the requirements of new generation aeroengine, it is necessary to develop an optimization method through which the final structural scheme of the rotor is determined.

Previous works on the optimum design of rotor system had been done by using transfer matrix method to calculate complex eigenvalues of the system [2–8]. Huang and Luo [2] analyzed the critical speed and unbalanced response of a rotor system using combined method (transfer matrix

and pseudomodal method) and changed the stiffness and dampness of the bearing to adjust critical speeds of the rotor. Choi and Yang [3] dealt with the optimum shape design of a rotor shaft. Equations of motion were established and solved to obtain the eigenvalues of the rotor and genetic algorithm was applied to determine the optimum diameters of the rotor shaft. Lee and Choi [4] analyzed a multistepped rotor supported by two angular contact ball bearings by using transfer matrix method and reduced the weight of the rotor through optimization. Huang and Lin [5] obtained the natural frequencies and the critical speeds of a typical rotor bearing system by solving the frequency equation in terms of receptances. The rotor's critical speeds were adjusted through optimizing parameters of supports. A low-pressure steam-turbine rotor was analyzed through calculation of eigenvalues and optimized by Yang et al. [6]. Under the constraints of shaft diameter, bearing length, and clearance, the resonance response of the second occurring mode in the excessive vibration was reduced after optimization.

During the design of modern aeroengines, the pursuit of high rotation speed, light weight, and high reliability leads

to much more complexity of the rotor system. Changing a single design parameter might cause multiple effects on the rotor system [1]. Simulation of rotordynamics and optimum design are becoming increasingly complicated because a large number of parameters need to be considered simultaneously. To solve this, finite element method (FEM) has been used to calculate rotor dynamics to obtain more accurate results on the one hand; multiobjective optimization of rotor system has been launched to fulfill all optimization objectives on the other hand. Minimal weight design optimization of a rotor system was formulated as a nonlinear constrained optimization problem by Pugachev in [9]. An in-house beam-based FEM code was used for the prediction of static and dynamic characteristics of the rotor system and a gradient projection method was used to solve the optimization problem. Using multiobjective optimization, Shiau et al. minimized a geared rotor-bearing system's quality, steady unbalance response, and transmission error response in [10]; Matthew and Patrick reduced a four-supporting rigid rotor's bearing vibration and disk's amplitude in [11]; Choi and Yang minimized the total weight and the transmitted forces at the bearings of a rotor-bearing system consisting of a single spool and three bearings in [12].

The previous works have contributed a lot for the optimization of rotor system. However, optimization algorithms and finite element codes used previously were generally in-house and not widely applicable in engineering rotor optimization. Additionally, the works reported in the literature rarely validated the optimum results through experimental data.

In this paper, a multiobjective optimization strategy based on the combination of commercial finite element software ANSYS and multidisciplinary optimization software ISIGHT is presented. ANSYS is used to calculate the dynamics of rotor system, and ISIGHT is used to solve the optimization problem. The interface between the two types of software is established. A laboratory scale two-disk flexible rotor test rig is established and optimized using the strategy. Experimental verification is carried out on the test rig. The disks' amplitudes and bearings' transmitted forces crossing the first critical speed are reduced significantly after optimization.

2. Optimization Strategy

A combined optimization strategy is proposed. The flow chart of the strategy is shown in Figure 1. The procedure of the strategy is as follows.

Step 1 (initial model establishment). This is the first step of the optimization strategy and finished in commercial finite element software ANSYS. It should be noted that the structural parameters of the rotor system which will be selected as optimization variables (parameters that can be changed in optimization, such as positions of bearings, positions of disks, stiffness of bearings, and size of the rotor shaft) should be modeled parametrically. Then dynamics of the rotor system can be obtained.

Step 2 (loading the model in ISIGHT). The two types of software, ANSYS and ISIGHT, are integrated in this step. Simcode assembly in ISIGHT, a command running with input data exchange and output data exchange, is used as the interface between the two types of software.

Step 3 (optimization problem formulation). Based on the dynamic characteristics of the rotor system obtained in Step 1, optimization objectives, design variables, and constraints are determined. The overall objective of the optimization is to reduce the vibration level of the rotor system. Since the most severe deformation occurs at the critical speed and the transmitted forces at two bearings reach the maximum at such a speed, the disks' amplitudes and the bearings' transmitted forces crossing the critical speed are chosen as optimization objectives. As the normal operating speed of the flexible rotor must be apart sufficiently far from its critical speed [1, 13], the critical speed should be limited to a certain range. In the present paper, the variation of the critical speed is controlled at the range of ±10%. After this step is completed, the optimization model has been set up. Selecting the optimization algorithm is also completed in this step. It needs to consider both the amount of calculation and the optimization performance when selecting a suitable optimization algorithm for the optimization problem. There are four kinds of multiobjective optimization algorithms in ISIGHT, including Hybrid Multigradient Pareto Explorer (PE), Archive-Based Microgenetic Algorithm (AMGA), Neighborhood Cultivation Genetic Algorithm (NCGA), and Nondominated Sorting Genetic Algorithm II (NSGA-II). In our previous work [14], a rotor system was optimized using those algorithms, respectively, to analyze the performance difference of the algorithms. NSGA-II presented the best optimization performance and acceptable computational cost. So in this paper, NSGA-II is chosen as the optimization algorithm.

Step 4 (DOE (Design of Experiment) analysis). DOE analysis is carried out to determine whether the optimization objectives are sensitive to the design variables and understand the variation tendency of optimization objectives [15, 16].

In ISIGHT, the results of DOE are postprocessed using quadratic regression model. The quadratic regression model of optimization problem is established based on sample points:

$$y = \beta_0 + \sum \beta_i x_i + \sum \beta_j x_j^2 + \sum_{i \neq j} \beta_{ij} x_i x_j, \tag{1}$$

where y is the optimization objective, x is the optimization variable, and β is the coefficient of the variable. The coefficient represents the main effect of every term (linear term, quadratic term, and interaction term) on the response of y. Taking two variables, for example, the regression model is given by

$$y = \beta_0 + \beta_1 x_1 + \beta_2 x_2 + \beta_3 x_1^2 + \beta_4 x_2^2 + \beta_5 x_1 x_2. \tag{2}$$
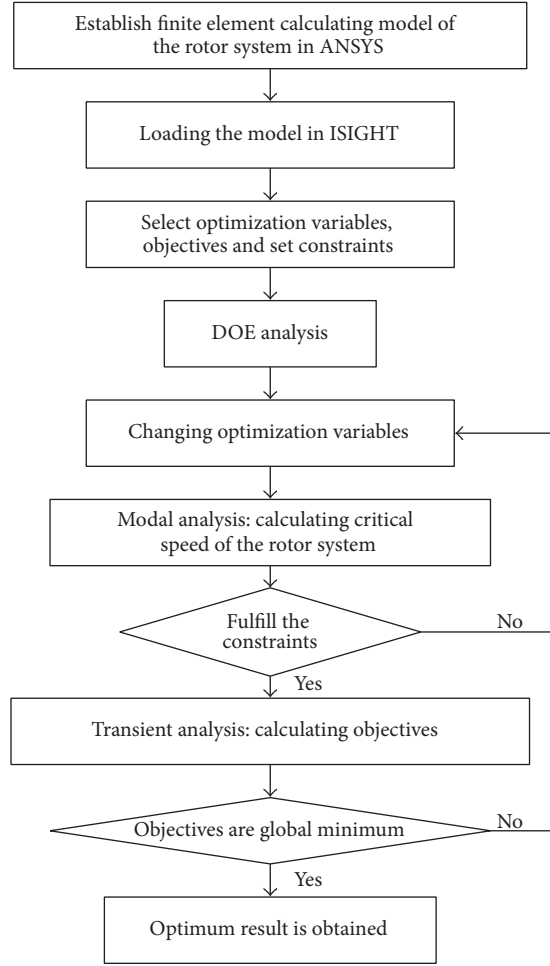
FIGURE 1: Flow chart of the optimization strategy.

The first derivative of y is

$$dy = \beta_1 dx_1 + \beta_2 dx_2 + 2\beta_3 x_1 dx_1 + 2\beta_4 x_2 dx_2 \\ + \beta_5 dx_1 x_2. \tag{3}$$

Thus, linear main effect of x_1/x_2 is

$$M_{x_1} = \beta_1 dx_1, \\ M_{x_2} = \beta_2 dx_2, \tag{4}$$

quadratic main effect of x_1/x_2 is

$$M_{x_1^2} = 2\beta_3 x_1 dx_1, \\ M_{x_2^2} = 2\beta_4 x_2 dx_2, \tag{5}$$

and interaction effect of x_1/x_2 is

$$M_{x_1 x_2} = \beta_5 dx_1 x_2, \tag{6}$$

where x, dx, and $dx_1 x_2$ are calculated as follows:

$$x = \frac{[\max(x) + \min(x)]}{2}, \\ dx = \frac{[\max(x) - \min(x)]}{2}, \tag{7} \\ dx_1 x_2 = [\max(x_1)\min(x_2) + \min(x_1)\max(x_2)] \\ - [\max(x_1)\max(x_2) + \min(x_1)\min(x_2)].$$

Since the range of each variable is different, variables are scaled to [−1, +1] to fairly reflect the contribution of every variable to the response. Then the main effect of every term is fitted by using a least-squares method. The main effect after fitting is presented as Pareto Graph.

Step 5 (iterative calculation). In this procedure, the values of objectives selected in Step 3 are changed according to NSGA-II. Then modal analysis will be performed to obtain the critical speed of the rotor system and to determine whether the critical speed fulfills the constraints. If fulfilled, transient analyses are performed to obtain objectives in current structure and then to determine whether the objectives
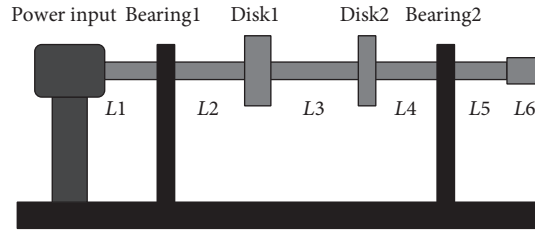
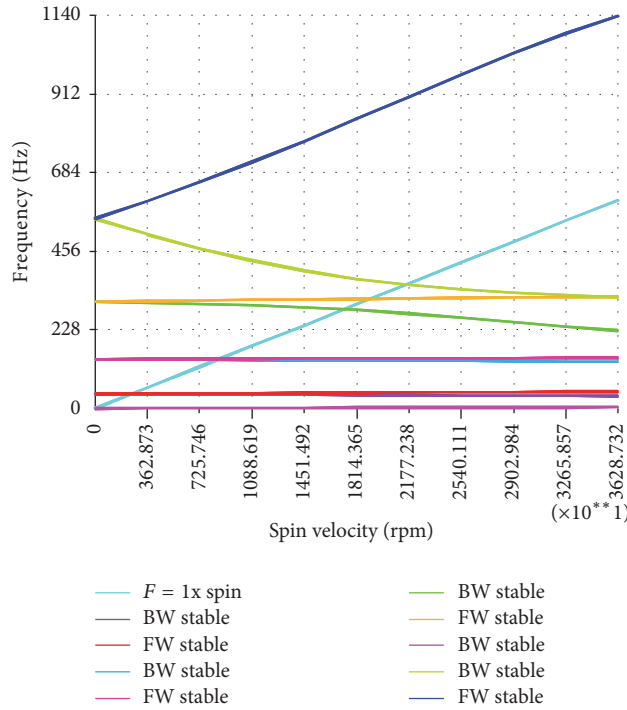FIGURE 2: Schematic structure of the two-disk flexible rotor system.

FIGURE 3: Campbell diagram of the rotor system.

are global minimum. If not, the values of variables are rechanged according to NSGA-II. The changed variables are then returned to the ANSYS input file to perform modal analysis and transient analysis again. The procedure is iterated to search possible optimum variables in which objectives become local minimum. After all possible optimum variables (i.e., Pareto front) are obtained, the optimum variables in which objectives become global minimum are chosen from Pareto front.

3. Optimization of the Two-Disk Flexible Rotor System

3.1. Two-Disk Flexible Rotor Test Rig. A two-disk flexible rotor test rig is designed and optimized. The schematic structure of the rotor system is shown in Figure 2.

The rotor system is composed of a rotating shaft, two disks (disk1 and disk2), and two supports (bearing1 and bearing2). The maximum speed is 10000 r/min. The diameter of the shaft is 0.009 m. It consists of 6 segments ($L1$ = 0.0515 m,

$L2$ = 0.109 m, $L3$ = 0.1485 m, $L4$ = 0.114 m, $L5$ = 0.0355 m, and $L6$ = 0.034 m). The thickness of disk1 is 0.019 m and its diameter is 0.076 m. The thickness of disk2 is 0.018 m and its diameter is 0.075 m. The installation position of disk1 and disk2 is 0.1835 m and 0.332 m from the left side, respectively (used as a baseline structure). The motor connected at the left side serves as power input of the entire rotor system.

Using rotordynamics calculation software ANSYS, the finite element model of the rotor system is established. Campbell diagram of the rotor system is obtained through modal analysis, which is shown in Figure 3. According to Figure 3, the first-order critical speed of the rotor system (represented by cs1) is 2925.5 r/min. Thus the constraints imposed on the critical speed are

$$2633 \leq \text{cs1} \leq 3218. \tag{8}$$

It is worth mentioning that the critical speed can be calculated directly by using ANSYS since the studied rotor system is isotropic. If orthotropic or anisotropic system is considered, ANSYS will be failing to calculate the critical speed; and
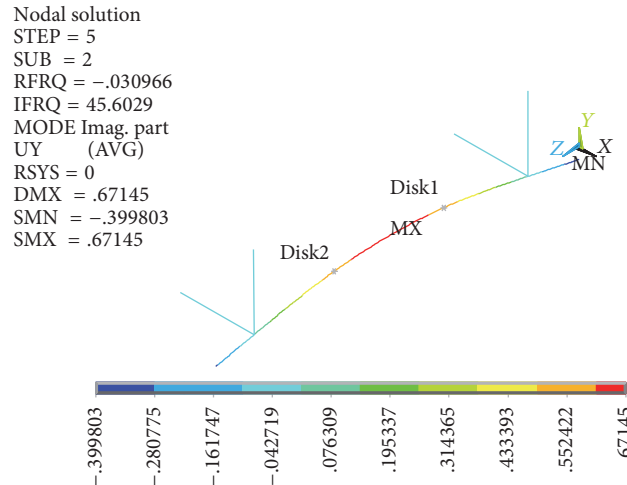
Nodal solution
STEP = 5
SUB = 2
RFRQ = −.030966
IFRQ = 45.6029
MODE Imag. part
UY   (AVG)
RSYS = 0
DMX = .67145
SMN = −.399803
SMX = .67145

Figure 4: The first-order mode shape of the rotor system.

more professional rotordynamics calculation software, such as SAMCEF for RORORO, is recommended.

Figure 4 shows the first-order mode shape of the rotor system. According to Figure 4, the first-order mode shape of the rotor system is flexure type. Reaching the first-order critical speed, the rotor will be flexibly deformed. The most severe deformation occurs at middle part of the rotor where disk1 and disk2 are located.

To obtain the dynamic responses of the rotor system, transient analysis (also known as time-history analysis) is carried out. The transient responses of the rotor system strongly depend on the distribution of unbalance mass along the rotor. Since the rotor system is balanced in advance, based upon the experience of balancing, the unbalance mass on disk1 is assumed 25.5 g·mm at 195 degree, and the unbalance mass on disk2 is assumed 17 g·mm at 57 degree. Transient characteristics of the rotor system are shown in Figure 5.

Transient analysis shows the maximum disks' amplitudes and bearings' transmitted forces are reached at the first order critical speed. At such a speed, the amplitude of disk1 and disk2 is $1.682e − 4$ m and $1.604e − 4$ m, respectively, and the transmitted force at bearing1 and bearing2 is 7.8849 N and 24.93 N, respectively.

The rotor system is then optimized using the proposed strategy to reduce its vibration level. The amplitude of the disk1 and disk2 (represented by a1 and a2, resp.) and the transmitted force of bearing1 and bearing2 (represented by f1 and f2, resp.) crossing the first-order critical speed are chosen as optimization objectives. Positions of the two disks (represented by Disk1_P and Disk2_P, resp.) are chosen as design variables. The rotor system's dynamic performance can be improved by adjusting the distribution of the rotor's mass and stiffness through changing the positions of the disks [13, 17].

3.2. Optimization. The initial position of disk1 and disk2 is, respectively, 0.1835 m and 0.332 m from the left side. Due to the limited moving range of disks in actual aeroengine rotor

system, the position of disk1 and disk2 is, respectively, left and right moving 0.01 m from initial position (i.e., Disk1_P changes in 0.1735 m~0.1935 m; Disk2_P changes in 0.322 m~0.342 m). Pareto Graphs obtained from DOE analysis are shown in Figures 6 and 7.

Figure 6 shows the effect of Disk1_P on optimization objectives. Figure 7 shows the effect of Disk2_P on optimization objectives. The values of every term in Pareto diagram are the main effect obtained from (4)–(7) after fitting. In Pareto Graph, the blue means positive effect and the red means negative effect [15]. If the proportion of linear term is greater than that of quadratic term, the relationship between variables and objectives is dominated by linear relationship.

Figure 6 shows that there is an approximately linear relationship between the position of disk1 and all of the objectives: decreasing the value of Disk1_P the value of a1, a2, f1, and f2 decreases, which is desirable in a minimization problem. Therefore, Disk1_P should be reduced in order to reduce a1, a2, f1, and f2. According to Figure 7, a1, f1, and f2 are increased as Disk2_P increases from 0.322 m to 0.342 m; however, a2 are decreased. That is to say, reducing Disk2_P can lead to a decrease in a1, f1, and f2 and an increase in a2.

In the present multiobjective optimization, the relative importance of each objective is of the same level, which means all the objectives should be minimized. In order to decrease the values of all the objectives, the values of Disk1_P and Disk2_P have a decrease tendency in the optimization process according to Figures 6 and 7. However, if the values of Disk1_P and Disk2_P are decreased to their minimum, the values of a1, f1, and f2 are decreased unsurprisingly, but the value of a2 may be increased because of the relationship of a2 and Disk2_P. To determine the optimum values of Disk1_P and Disk2_P, multiobjective optimization is carried out using NSGA_II. Optimization result is shown in Table 1.

As can be seen from Table 1, the values of a1, a2, f1, and f2 are decreased by 11%, 2%, 5%, and 8%, respectively, after optimization. What is more, the values of Disk1_P and Disk2_P are decreased but not reaching their minimum, which agrees well with the DOE analysis results.
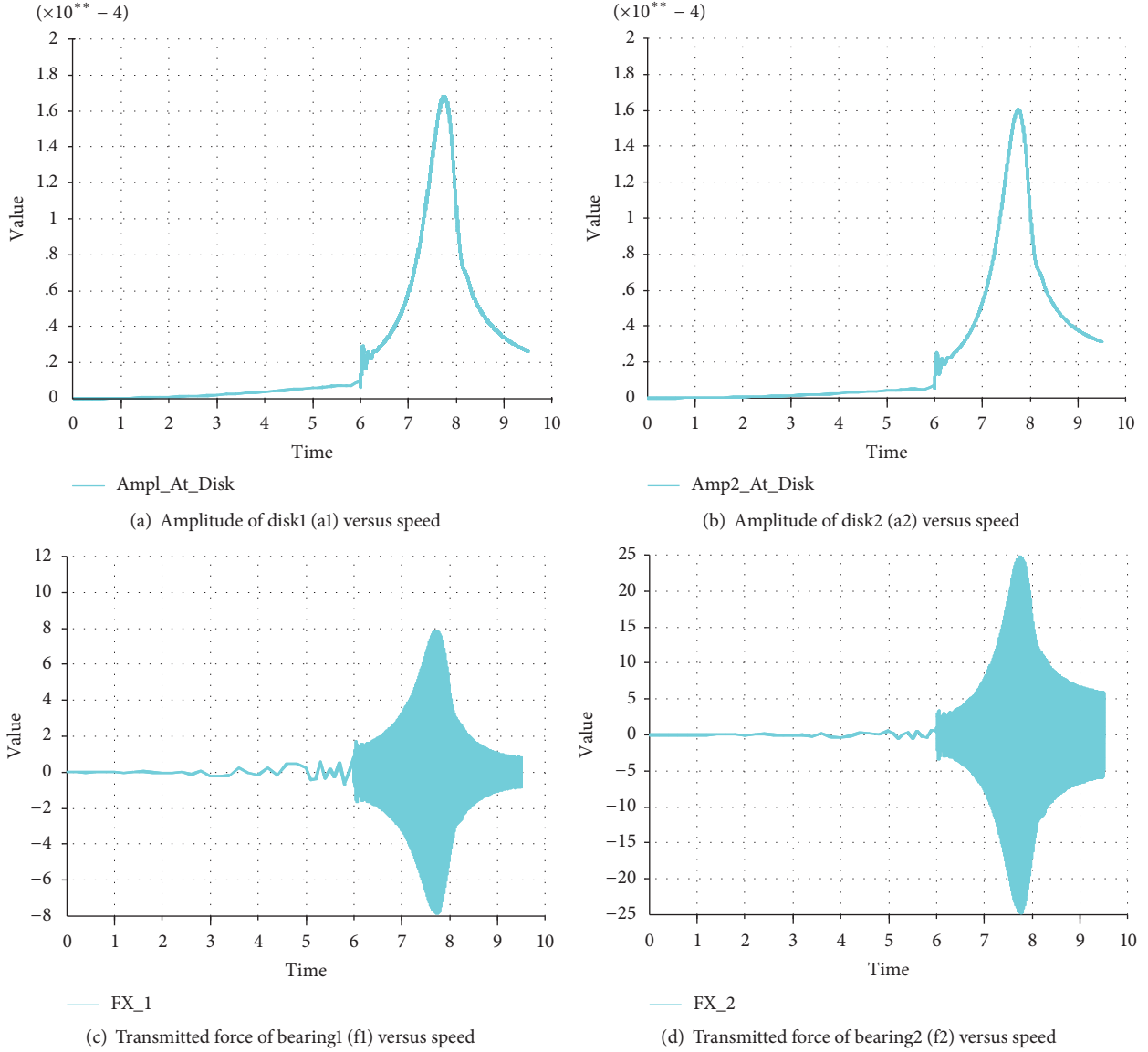
$(\times 10^{**} - 4)$

(a) Amplitude of disk1 (a1) versus speed

$(\times 10^{**} - 4)$

(b) Amplitude of disk2 (a2) versus speed

(c) Transmitted force of bearing1 (f1) versus speed

(d) Transmitted force of bearing2 (f2) versus speed

Figure 5: Transient responses of the rotor system.

Table 1: Numerical optimization result of Disk1_P and Disk2_P.

	Disk1_P/m	Disk2_P/m	a1/$e-4$ m	a2/$e-4$ m	f1/N	f2/N	cs1/(r/min)
Baseline	0.1835	0.332	1.682	1.6044	7.8849	24.93	2926
After optimization	0.178	0.324	1.5	1.58	7.47	23.07	2851

4. Experimental Results and Discussion

To verify the validity of the numerical optimization results, experiments are carried on the test rig shown in Figure 8.

A photoelectric sensor is used to capture the rotor shaft's rotation speed, two TR81 eddy current displacement sensors are used to measure the two disks' amplitudes, and two integrated circuit piezoelectric acceleration sensors are used to measure the two bearings' accelerations.

Move Disk1_P from initial 0.1835 m to optimized 0.178 m and move Disk2_P from initial 0.332 m to optimized 0.324 m.

Amplitudes of the disks and transmitted forces at the bearings before and after optimization are compared in Figure 9.

The longitudinal axis of Figures 9(c) and 9(d) is voltages of the bearings' vibration acceleration which are directly measured by the acceleration sensors. Because there is a linear relationship between the voltages of the vibration acceleration and the magnitudes of transmitted forces at the bearings, such voltages are used to characterize the vibration of bearings.

In Figure 9, dashed lines represent the transient response before optimization and solid lines represent the response
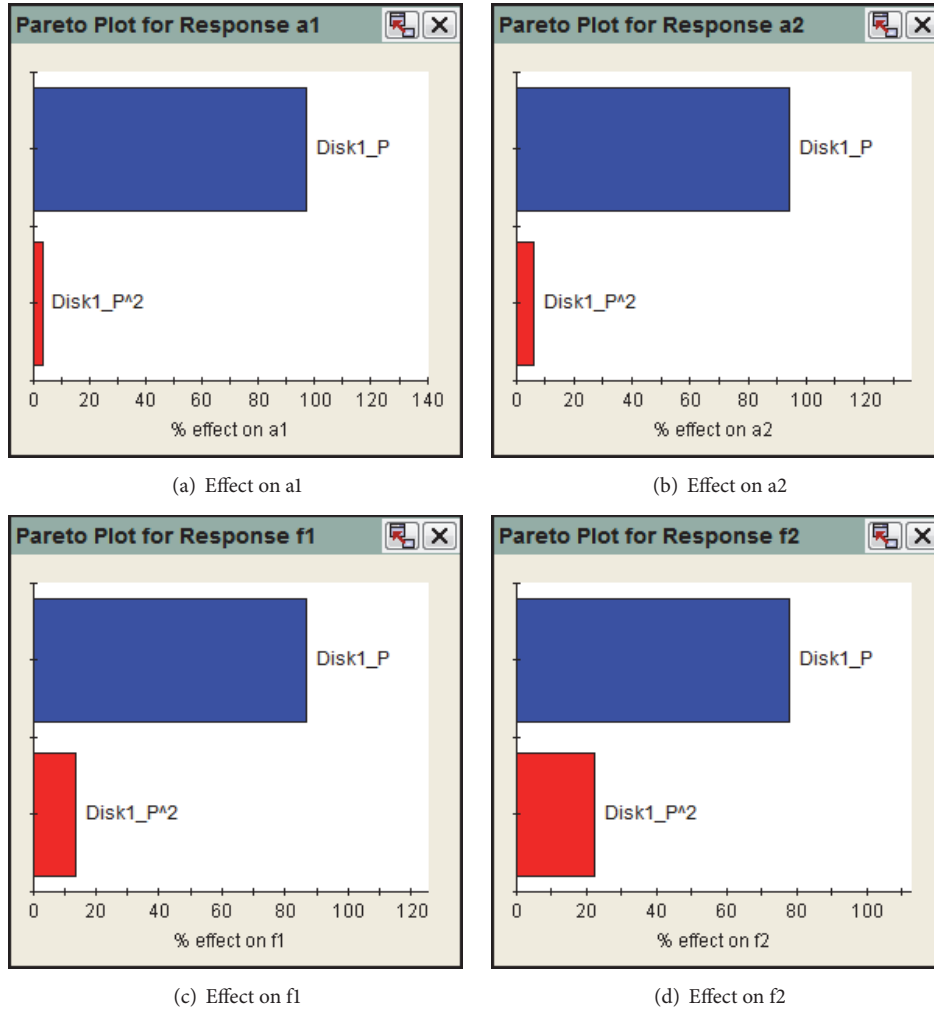
(a) Effect on a1

(b) Effect on a2

(c) Effect on f1

(d) Effect on f2

Figure 6: Effect of changing Disk1_P on optimization objectives.

Table 2: Experimental optimization result of Disk1_P and Disk2_P.

	Disk1_P/m	Disk2_P/m	a1/$e-4$ m	a2/$e-4$ m	v1/V	v2/V	cs1/(r/min)
Baseline	0.1835	0.332	1.79	1.485	3.43	4.35	2916
After optimization	0.178	0.324	1.114	1.317	2.45	3.7	2959

after optimization. According to Figure 9, experimentally measured first-order critical speed of the rotor system before optimization is 2916 r/min, while the numerical value according to Figure 3 is 2925.5 r/min. The difference between the numerical simulation and experiment data is 0.33%, validating the initial calculating model established in ANSYS.

Optimization result obtained from experimental data is shown in Table 2.

In Table 2, v1 represents the voltage of bearing1 corresponding to f1, and v2 represents the voltage of bearing2 corresponding to f2. The comparison between Tables 1 and 2 shows that the values of a1 and a2 obtained from numerical simulation and experiment have little difference, which also validates the initial calculating model established in ANSYS.

According to Table 2, at the optimized positions of disk1 and disk2, the values of a1 and a2 are decreased by 36% and 11%, respectively; the values of v1 and v2 are decreased by 28.6% and 14.9%, respectively. The optimization effectiveness of this strategy is significant.

As can be seen from the comparison between Tables 1 and 2, experimental reductions of the objectives are generally greater than numerical reductions. The main cause of this error is that the transient characteristics of the rotor-bearing system obtained by numerical calculation and experiments are not accurately consistent because the distribution of unbalance mass along the rotor is unknown [18]. Certain unbalance mass is imposed on the system in order to excite transient response when performing numerical calculation.

(a) Effect on a1

(b) Effect on a2

(c) Effect on f1
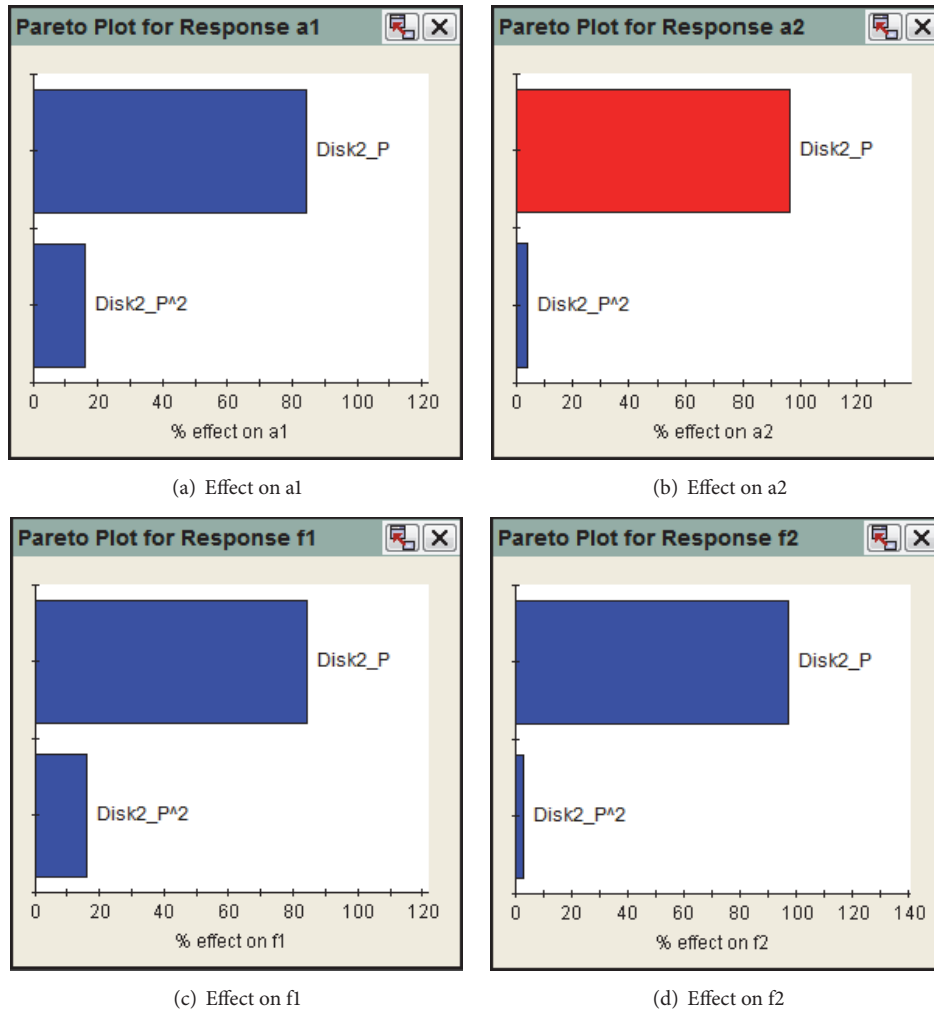

(d) Effect on f2

Figure 7: Effect of changing Disk2_P on optimization objectives.
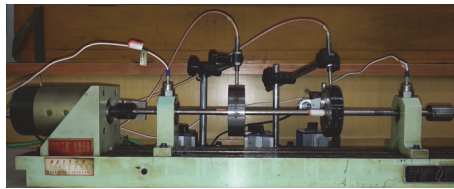

Figure 8: Test rig of the two-disk flexible rotor system.

In this paper, the unbalance mass on disk1 is assumed 25.5 g·mm at 195 degree, and the unbalance mass on disk2 is assumed 17 g·mm at 57 degrees, while in the experiment the real distribution of unbalance mass is not like the assumption one. That is to say, the numerical results are obtained based on the hypothetical distribution of unbalance mass, while the experimental results are obtained based on the real distribution of unbalance mass. Much effort is needed to perform robust optimization based on the uncertainty of residual unbalance, which is our future work.

5. Conclusions

In this paper, a multiobjective optimization strategy is presented to reduce the vibration level of a flexible rotor system. A laboratory scale two-disk flexible rotor system is established and optimized using the proposed strategy. Experimental results of transient response before and after the optimization show that the vibration level of the rotor system is reduced significantly after optimization. The amplitudes of the two disks are reduced by 36% and 11%, and

(a) Transient response of a1

(b) Transient response of a2

(c) Transient response of f1
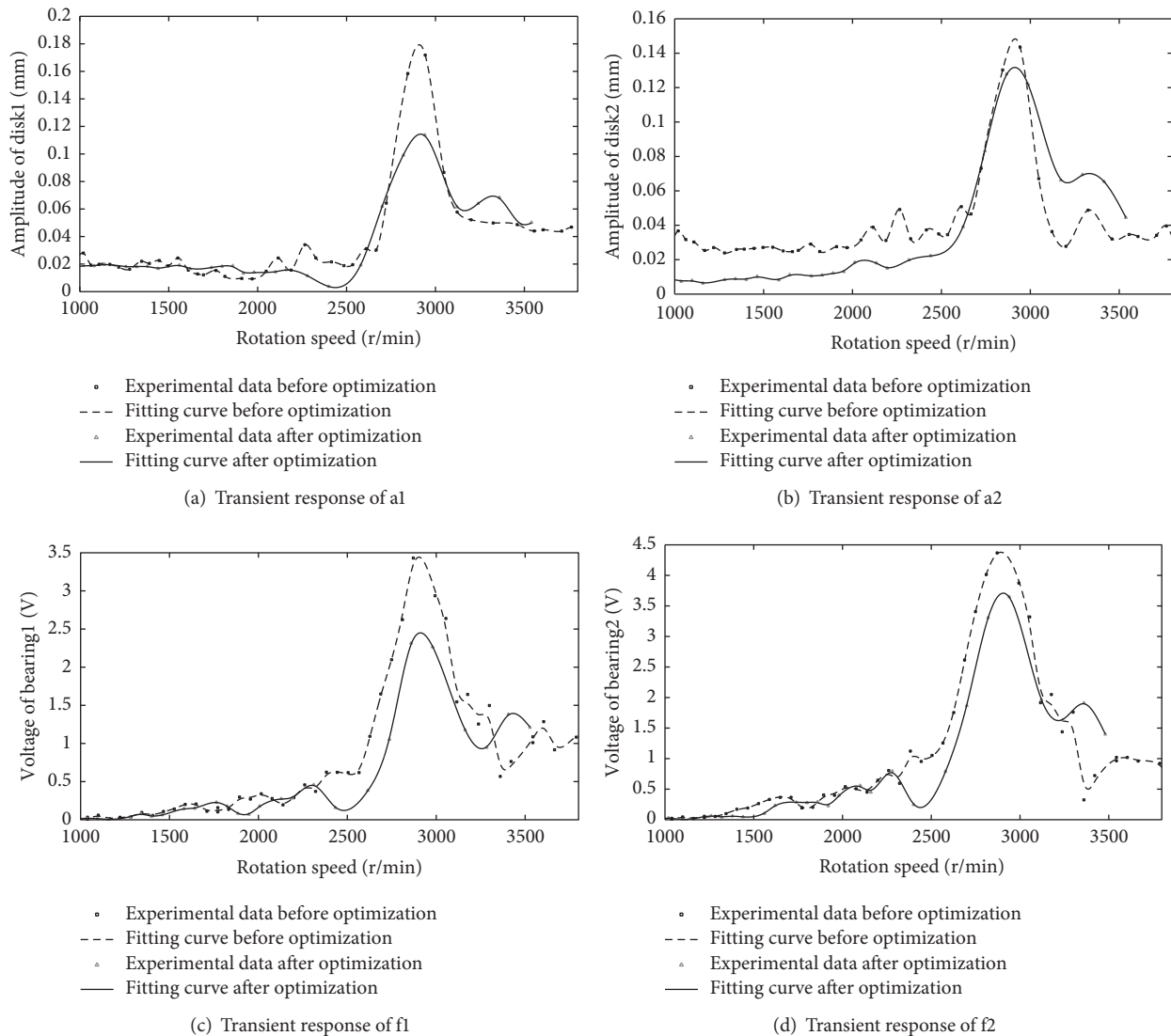
(d) Transient response of f2

FIGURE 9: Transient response before and after optimization of Disk1_P and Disk2_P.

the transmitted forces at the two bearings are reduced by 28.6% and 14.9%, respectively. The experimental data supports the effectiveness of the proposed optimization strategy. The optimization strategy proposed in this paper can be an inspiration and reference for engineering rotor design.

Competing Interests

The authors declare that they have no competing interests.

Acknowledgments

References

[1] H. B. Zhang, Z. G. Li, and J. Chen, *Design Manual of Aircraft Engine Machine*, Aviation Industry Press, Beijing, China, 2000 (Chinese).

[2] T. P. Huang and G. L. Luo, "Dynamic optimization design of the rotor," *Journal of Aerospace Power*, vol. 9, no. 2, pp. 113–116, 1994 (Chinese).

[3] B. G. Choi and B. S. Yang, "Optimum shape design of rotor shafts using genetic algorithm," *Journal of Vibration and Control*, vol. 6, no. 2, pp. 207–222, 2000.

[4] D.-S. Lee and D.-H. Choi, "Reduced weight design of a flexible rotor with ball bearing stiffness characteristics varying with rotational speed and load," *Journal of Vibration and Acoustics*, vol. 122, no. 3, pp. 203–208, 2000.

[5] S.-C. Huang and C.-A. Lin, "Sensitivity analysis and optimization of undamped rotor critical speeds to supports stiffness,"

Journal of Vibration and Acoustics, Transactions of the ASME, vol. 124, no. 2, pp. 296–301, 2002.

[6] B. S. Yang, S. P. Choi, and Y. C. Kim, "Vibration reduction optimum design of a steam-turbine rotor-bearing system using a hybrid genetic algorithm," *Structural and Multidisciplinary Optimization*, vol. 30, no. 1, pp. 43–53, 2005.

[7] F. Strauß, M. Inagaki, and J. Starke, "Reduction of vibration level in rotordynamics by design optimization," *Structural and Multidisciplinary Optimization*, vol. 34, no. 2, pp. 139–149, 2007.

[8] D. H. Wang, Z. S. Liu, and W. Dou, "Design optimization of rotor system based on hybrid genetic algorithm," *Journal of Vibration and Shock*, vol. 28, no. 5, pp. 87–91, 2009 (Chinese).

[9] A. O. Pugachev, "Application of gradient-based optimization methods for a rotor system with static stress, natural frequency, and harmonic response constraints," *Structural and Multidisciplinary Optimization*, vol. 47, no. 6, pp. 951–962, 2013.

[10] T. N. Shiau, J. R. Chang, and W. B. Wu, "Multilevel optimization of the geared rotor-bearing system for multi-objectives with critical speed constraints," in *Proceedings of the ASME Turbo Expo 2004 Power for Land, Sea, and Air*, pp. 14–17, Vienna, Austria, June 2004.

[11] O. T. C. Matthew and S. K. Patrick, "On LMI-based optimization of vibration and stability in rotor system design," in *Proceedings of the ASME Turbo. Expo. 2005: Power for Land, Sea and Air*, pp. 6–9, Reno-Tahoe, Nev, USA, 2005.

[12] B.-K. Choi and B.-S. Yang, "Multiobjective optimum design of rotor-bearing systems with dynamic constraints using immune-genetic algorithm," *Journal of Engineering for Gas Turbines and Power*, vol. 123, no. 1, pp. 78–81, 2001.

[13] J. L. Gu, *Rotor Dynamics*, Defence Industry Press, Beijing, China, 1985.

[14] J.-J. Huang, L.-X. Zheng, G.-Q. Liu, and Q. Mei, "Optimization algorithm and experiment of a two-disk rotor system," *Journal of Aerospace Power*, vol. 31, no. 1, pp. 65–71, 2016 (Chinese).

[15] Y. Y. Lai, X. Jiang, and L. Q. Fang, *Parameter Optimization Theory and Explain Examples with Isight*, Beihang University Press, Beijing, China, 2012.

[16] D. H. Wang and Z. S. Liu, "Rotor structure optimal design based on genetic algorithm," *Turbine Technology*, vol. 47, no. 6, pp. 407–410, 2006 (Chinese).

[17] Y. E. Zhong, *Rotor Dynamic*, Tsinghua University Press, Beijing, China, 1987.

[18] C. D. Untaroiu and A. Untaroiu, "Constrained design optimization of rotor-tilting pad bearing systems," *Journal of Engineering for Gas Turbines and Power*, vol. 132, no. 12, Article ID 122502, 7 pages, 2010.